Desalination and Water Treatment
www.deswater.com

36 (2011) 363–373
December

1944-3994/1944-3986
doi: 10.5004/dwt.2011.2421

The effects of feed water temperature and dissolved gases on permeate flow rate and permeate conductivity in a pilot scale reverse osmosis desalination unit

M.J. Francis[a*], R.M. Pashley[b]

[a]*Curtin Water Quality Research Centre, Curtin University, Perth, Australia. Tel: +618 92662743; Fax: +618 92662300; Email: m.francis@curtin.edu.au*
[b]*University of New South Wales, Australian Defence Force Academy, Canberra, Australia*

ABSTRACT

Feed water temperature is an important parameter in determining the optimum conditions for an efficient seawater reverse osmosis (SWRO) process. Increased feed water temperatures are known to increase the permeate flux rate in commercial SWRO systems. There are several factors which link feed water temperature to the operational efficiency of the fundamental membrane desalination process. In this study we have obtained precise data on these effects using two different types of RO membranes in a small scale pilot unit with feeds of seawater, brackish water and pure water. The mechanisms involved have been examined in this work. Pre-heating the feed water to enhance RO efficiency may lead to greater cavitation within the RO membrane. Vapour cavities formed by cavitation have the potential to hinder permeate flow by blocking sections of the polymer matrix in the skin layer of the membrane. In earlier work, it was identified that the presence of dissolved atmospheric gases in seawater leads to a potential for cavitation within the porous membranes used in high pressure RO processes. It was also established that the almost complete removal of these dissolved gases prevented this cavitation. The effects of de-gassing on the permeate rate in a small scale pilot SWRO system was reported recently. This work has been extended here to include more hydrophobic membranes, which are more likely to produce cavitation. In addition, there is new evidence to support the view that de-gassing the feed water can remove/reduce vapour cavities in the membrane for improved flow, which is maintained even when the feed water is re-gassed.

Keywords: Desalination; Degassing; Temperature effects

1. Introduction

It has been reported that in commercial seawater reverse osmosis (SWRO) plants there is a significant benefit in using a raised feed water temperature [1]. There appears to be an optimum temperature of around 30°C, for some industrial plants [2]. The main effect of raising feed water temperature is to increase the permeate flow rate, typically by about 2–3% per °C in the range 20–30°C [3]. This represents a significant cost and energy saving, if the heat required can be obtained either from environmental conditions or from waste industrial heat. It is therefore important to understand how the feed water temperature affects the permeate rate, as well as other properties of the SWRO system.

From basic physical chemistry, it might be expected that feed water temperature could potentially affect many parameters important for membrane desalination. The skin layer of commercial RO membranes is

*Corresponding author

typically thin, at about 0.1–0.2 μm [4]. Hence, it follows that the water within this skin layer will be thermally equilibrated with the feed water, that is, the membrane water will be at the same temperature as the feed water solution. Thus, any membrane effects caused by changing the feed water temperature will not be related to any difference in water chemical potential between the feed water and the membrane water. In RO membrane processes, changes in feed water temperature are expected to affect all of the factors listed below, which might be expected to affect membrane efficiency to varying degrees [5].

- Water viscosity and feed water solution viscosity.
- Water vapour pressure and feed water solution vapour pressure.
- Dielectric constant of water in the membrane.
- Ion diffusion rate.
- Ion hydration.
- Water–water molecular interaction.
- Membrane swelling or expansion.
- Osmotic pressure of the feed solution at the membrane surface.
- Thickness of the fluid boundary layer next to the membrane.

It is useful to estimate the likely magnitude of each of these effects in RO membrane separation processes, in the practical range of between 20 and 30°C. If we make the initial approximation that only pure water passes into the RO membrane skin layer, then the effect of temperature on the viscosity of pure water will be an important factor in determining permeate flow. Although the skin layer of an RO membrane actually consists of a porous polymer matrix with water-filled channels, it is interesting to apply the simple capillary flow model of Hagen-Poiseuille (H-P) [6]. The H-P equation (Eq. (1)) predicts that the flow rate (V_f) through an ideal cylindrical pore will depend on pore geometry (of radius r and length l), the applied pressure gradient ($\triangle P$) and the dynamic viscosity (η) of the fluid and is given by the relation:

$$V_f = (\pi \Delta P^4)/8\eta l, \tag{1}$$

which indicates that the flux through an RO membrane will depend critically on pore size but also that the flux will be increased by a reduction in pure water viscosity. Between 20 and 30°C the viscosity of pure water falls fairly linearly, at a rate of about 2%/°C, in reasonable agreement with reported observations on the membrane flux of commercial SWRO plants. Many of the other factors listed above must also affect flux rate but it appears that viscosity effects dominate [7]. Given the molecular complexity of the membrane transport process, it is, perhaps, surprising that such a simple model should work so well.

Some of the other factors can be readily discarded as insignificant, for example, the dielectric constant of water is a weaker function of temperature, decreasing 5% in the 20–30°C range and the latent heat of vaporization of water only changes 1% over this temperature range [8]. Changes in ion hydration and polymer expansion are also insignificant over this temperature range. Although any polymer expansion or swelling will increase the effective pore radius and increase flow rate at the cost of reduced salt rejection efficiency. Osmotic pressure is a linear function of the absolute temperate and so only changes about 0.3%/°C. By comparison, the vapour pressure of water increases rapidly between 20 and 30°C, almost doubling in value. This suggests that liquid water is present within the polymer matrix and that the transport process does not involve the transient vaporisation of water.

The reduction in (feed) solution viscosity with temperature should also enhance ion diffusion and hence reduce concentration polarization at the membrane surface. This will reduce the osmotic pressure at the membrane surface (π_m) and hence will increase the effective cross membrane pressure ($\triangle P$), since this is given by the applied pressure ($\triangle P_a$) minus the osmotic pressure at the surface of the membrane (π_m):

$$\Delta P = \Delta P_a - \pi_m \tag{2}$$

Another important parameter is the effect of temperature on salt rejection levels. The Born ion hydration model [9] can be used to give a fundamental explanation for the salt rejection behaviour of polymer RO membranes. In this model it is assumed that ions are rejected from the porous membrane structure because of its local environment of lower dielectric constant, relative to that of the feed water solution. It may also be possible to use this model to explain some of the effects of feed water temperature on salt rejection levels. The (Born) energy difference ($\triangle E$) between an ion just within the membrane and in bulk solution next to the membrane surface inhibits the ions from entering the membrane. This effect is opposed by the concentration difference developed between the feed solution (C_i^f) and the solution within the membrane (C_i^m). The balance of these two opposing effects leads to a Boltzmann distribution of the form:

$$C_i^m = C_i^f \exp\left(-\frac{\Delta E}{KT}\right) \tag{3}$$

where the energy difference ($\triangle E$) can be estimated from the Born energy required to transfer an ion from

bulk solution into the membrane skin layer. This energy is given by the Born Eq. (4) [9]:

$$\Delta E = \frac{(zq_e)^2}{8\pi\varepsilon_0 a}\left[\frac{1}{\varepsilon^0_m} - \frac{1}{\varepsilon^0_W}\right] \quad (4)$$

where z is the valency of the ion, q_e the electronic charge and a the radius of the ion. ε_0 is the permittivity of free space and $\varepsilon^0{}_m$ and $\varepsilon^0{}_w$ correspond to the static dielectric constants of the membrane skin layer and the feed solution, respectively. The value $\varepsilon^0{}_m$ can be identified as an 'effective' dielectric constant seen by the ions within the skin layer of the membrane.

As an example, for a standard, single stage, commercial RO membrane, Na^+ ions (Pauling radius = 0.095 nm) are rejected at a ratio of about 1/20 (i.e., 95% salt rejection level). From Eq. (3) this corresponds to a value of $\triangle E$ of about 3 kT. At 20°C seawater has a static dielectric constant of about 70 [10] which in Eq.(4) gives an effective membrane dielectric constant of about 40. This is the effective dielectric environment sensed by these ions. This method has been applied to the analysis of the salt rejection levels observed in this study.

In order to get a more detailed picture of these effects, the current study has examined the effects of feed water temperature on permeate flux for two quite different membranes, Filmtec™ (thin film composite polyamide/polysulfone/polyester) membranes and cellulose acetate membranes, with seawater, brackish water and pure water.

It has been suggested that the presence of dissolved atmospheric gases in the feed water in combination with the steep pressure release across the skin layer of an RO membrane, might produce cavitation within the membrane surface, which might reduce the permeate rate [11]. An earlier study demonstrated that the rapid application and release of applied pressures in the range of 10–60 atm caused visible cavitation in bulk solution phase [12]. This phenomenon was not related to increased gas solubility under the applied pressure, since no additional gases were allowed into the system. Furthermore, it was found that almost complete removal of the initial dissolved atmospheric gases prevented this cavitation [12]. Earlier laboratory scale studies had reported that removal of cavitation by feed water de-gassing enhanced permeate flow rates by 3–5% [11] but this level of improvement was not observed in the more recent pilot scale study operating at applied pressures of about 38 atm, with seawater feed [12]. This work has been extended in the present study using a more hydrophobic membrane, which is more likely to be susceptible to this cavitation effect.

Commercial RO membranes contain surfactant coatings, apparently to facilitate complete wetting during set up [12]. A series of studies was carried out to determine if the use of de-gassed feed water could facilitate wetting or the removal of vapour cavities in the polymer matrix in both new Filmtec™ membranes and those which had been used but never exposed to de-gassed feed water.

2. Methods and materials

Consistent sources of treated brackish water and seawater could not be sourced for the experiments reported here. Therefore, the feed water used for this study was either a salt solution of seawater (0.5 M) or brackish water (0.2 M) concentration. The salt solutions were made by mixing tap water and flossy curing salt (West Australian Salt Refinery) which has a 99.9% purity of NaCl. The 0.5 M solution had an average measured conductivity of 45.1 ± 2 mS/cm. The 0.2 M solution had an average measured conductivity of 26.61 mS/cm. The chlorine level was monitored using an ORP probe (TPS Aqua-pH with redox sensor) and was kept below 175 mV, using sodium metabisulphite, to protect the membrane. The feed water was stored in a 28 m^3 tank, and pH and conductivity were found to maintain their original values for up to three months, during storage. The water was pumped from the tank using a Davey Torrium centrifugal pump. It was then fed through a Waterco Micron W300 MkII sand filter, and a membrane microfilter, to protect the reverse osmosis membrane, by removing any suspended solids. The feed water was then delivered to a pair of Liquicel 4 × 28 hollow fibre modules, with ×50 fibres, arranged in series.

During the tests with the degassed feed water, a vacuum was applied to the hollow fibre membranes, with an Edwards E2M40 two stage rotary vacuum pump. Vacuum pressure was monitored using an Endress-Hauser Cerabar-S digital pressure gauge, the gauge measured in kPa to two decimal places (quoted error ± 0.075%) [13]. The dissolved oxygen level and temperature of the feed water was recorded as it left the hollow fibres, using a Mettler-Toledo InPro 6900 trace-level dissolved oxygen probe, connected to an M700 transmitter.

The feed water was then delivered to a high pressure, three-cylinder Catpumps 1057 Triplex pump, driven by a 4 kW Monarch Alloy electric motor, which was controlled by a Santerno Sinus M variable frequency drive, allowing the pump speed to be varied and controlled precisely. A pulsation damper was used to limit rapid pressure variations from the piston pump. Industrial scale RO plants more commonly use centrifugal pumps to push water through the

membranes; however, centrifugal pumps are not readily available for small-scale systems, such as this one. Therefore, a triple piston pump was used in this pilot study. Use of this type of pump also enabled us to control the flow-rate, via the piston frequency, separate to the applied pumping pressure. This pump was used to pressurise the feed water to pressures of up to 64 atm, which was then delivered to a Filmtec™ SW30-4040 reverse osmosis membrane (surface area of 7.4 m^2), housed in a Codeline fibreglass pressure vessel. A needle valve was used to generate and control the pressure by restricting the reject output flow. A bypass valve was used to allow low-pressure rinsing of the system.

The feed pressure was measured in the sand filter, and in the feeds to the hollow fibre modules and the high pressure pump, to a precision of ± 0.1 atm, and in the reverse osmosis membrane, to a precision of ± 0.5 atm, with Wika mechanical pressure gauges. The flow rate was monitored at the inlet to the hollow fibre modules, and at the reject outlet from the reverse osmosis system, using Bürkert digital flow meters. The Bürkert flow meter measured in m^3/hr (for feed and reject flows) to two decimal places or L/hr to one decimal place (for permeate flow). The quoted error for the flow meters was $\pm 0.5\%$. The pressure difference between the high-pressure reverse osmosis inlet and high-pressure reject streams was monitored with an Endress-Hauser Databar-S digital pressure gauge.

Unfortunately, it was found that the high-pressure pump created slight (i.e. a few %) variation in both feed rate and pressure. These pressure pulsations occurred even though the pump system was fitted with a pulse damper. This effect caused the flow meters to fluctuate. Because of this problem, the permeate flow rate was measured both using the flow meter and also by diverting the permeate stream into a temporary storage vessel, where its weight could be continuously monitored — giving short-run flow rates (typically over 5 min intervals). This allowed a more accurate time weighted average of the permeate flow rate to be collected.

During runs, the reject flow was stored in a 10 m^3 holding tank, until the end of each experiment, whereupon the permeate was also added to this tank. After each experiment, the mixed content of this tank were returned to the 28 m^3 storage tank, by means of a Davey Dynapump centrifugal pump. A schematic of the entire process is presented in Fig. 1.

The experiments involving the cellulose triacetate membrane (4040-SB20-TSA Trisep – surface area 7.4 m^2) were run at a feed water pressure of 30 atm, as the maximum safe working pressure of the membrane was 34 atm. Experiments involving the Filmtec™ membranes were run at feed water pressures of 38 atm as this yields a similar recovery rate per module to that currently used in industry. Baselines were also determined prior to degassing runs as initial flow rates through new membranes can be inconsistent. Each run was begun by bypassing the needle valve pressure control, and rinsing the system with the treated seawater feed, using only the low pressure Davey feed pump. The output flows were diverted to waste, until no flow was observed from the permeate line. This indicated that the membrane was filled with high osmotic pressure seawater, at which point, the output flows were diverted back to the 10 m^3 holding tank. The high-pressure, reverse-osmosis pump was then activated, and the needle-valve bypass was closed. The high-pressure pump speed and needle valve were adjusted until the desired flow rate and feed pressure were achieved. The system was then run for 90 min, with measurements being taken every 5 min. After the conclusion of the measurements, the pressure was reduced, the needle valve bypassed, and the pumps switched off. For storage, the system was rinsed with tap water, which was treated with sodium metabisulphite, to prevent damage to the membranes due to residual chlorine in the tap water.

A similar method was used for the experiments with degassed feed. The system was run with the same procedure as before for the first 30 min of each 90 min experiment. After 30 min, the vacuum pump was switched on to produce a vacuum on one side of the hollow fibre membranes. A vacuum level of about 1 kPa or lower was typically achieved within about 10 min. This corresponds to a de-gassing level of 99% or better. The actual de-gassing level achieved with time was monitored continuously using a dissolved oxygen (DO) probe. After 30 min of degassed operation, the vacuum was removed, and the hollow fibres were vented to the atmosphere. The DO levels returned to atmospheric levels within a 5–10 min. The system was then run for a further 30 min under gassed conditions. This method allowed the performance of the system under gassed conditions to be contrasted directly with the performance of the system under degassed conditions, gained under otherwise identical conditions. Degassed experiments were performed at feed water pressures of 38 atm for Filmtec™ membranes and 30 atm for Cellulose Acetate (CA) membranes. When the vacuum pump was used, water vapour was transferred across the hollow fibre membrane with the dissolved atmospheric gases. At these low vacuum pressures, the water vapour acts as a carrier gas for the other atmospheric gases. To protect the vacuum pump, several traps filled with pre-dried silica gel were set up just before the inlet to the vacuum pump. The silica gel in these traps had to be replaced regularly.

The experiments which observed the change in flux rate with temperature were run by remixing the

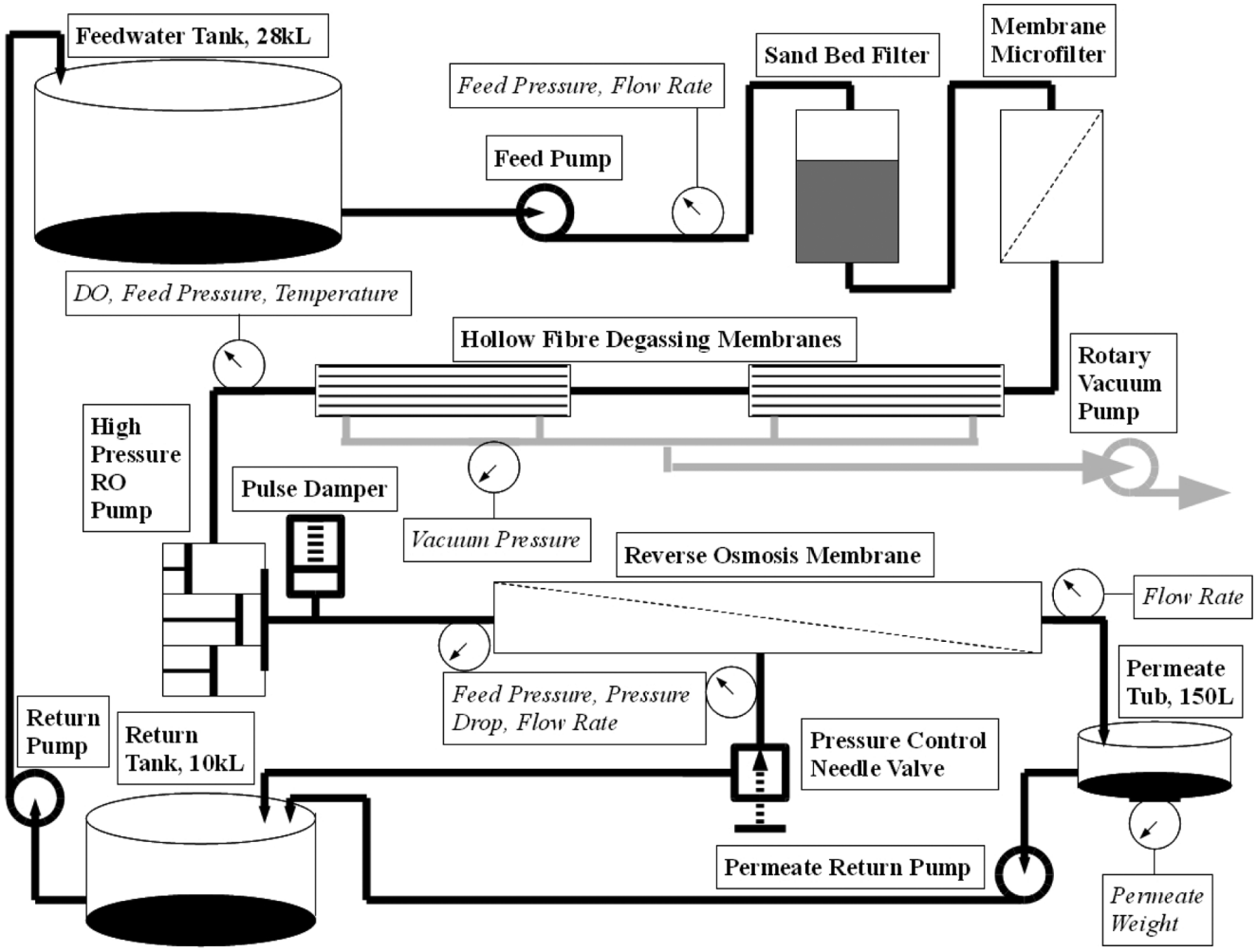

Fig. 1. Schematic of Reverse Osmosis pilot system used in this study.

permeate and reject into a 60 L water tank. This water was then pumped back through the sand filter and through the RO membrane. The high pressure pump added enough heat to the recirculating water that the feed water temperature would increase by 15° in four hours. This allowed permeate flow measurements to be taken every 0.5°C. Two temperature runs were carried out at 10 atm using the rinse water (tap water dosed with sodium metabisulphite) as the feed solution. This was to compare the temperature characteristics of Filmtec™ and CA. The change in temperature was monitored using a Traceable Digital Thermometer (Control Company Cat No. 4000). The resolution of the digital thermometer was 0.001°C with an accuracy of 0.05°C between 0 and 100°C.

3. Results and analysis

The permeate flow rate was monitored with increasing temperature for the Filmtec™ membranes at applied feed pressures of 10, 40, 50 and 60 atm. The feed water used in these experiments was a premixed 0.5 M NaCl solution, made up from tap water. Sodium metabisulphite (0.0025% w/w) was added to remove chlorine. The resulting effects of increase in feed water temperature on recovery rate, permeate flow as a % of feed flow, at each pressure, are given in Fig. 2. A fairly linear increase in recovery rate was observed at all the applied pressures over a temperature range of 16–32°C.

Permeate flow rates were also measured with increasing temperature using the Cellulose Acetate membranes at 10 atm (with rinse water feed at an approximate concentration of 0.005–0.01 M NaCl and at 30 atm with brackish water (at about 0.2 M NaCl). The results are presented in Fig. 3. Again, a linear increase was observed with temperature. The rate at which the recovery rate changed with temperature was found to be lower with CA than it was for Filmtec™, for the same feed water. Typical results comparing CA

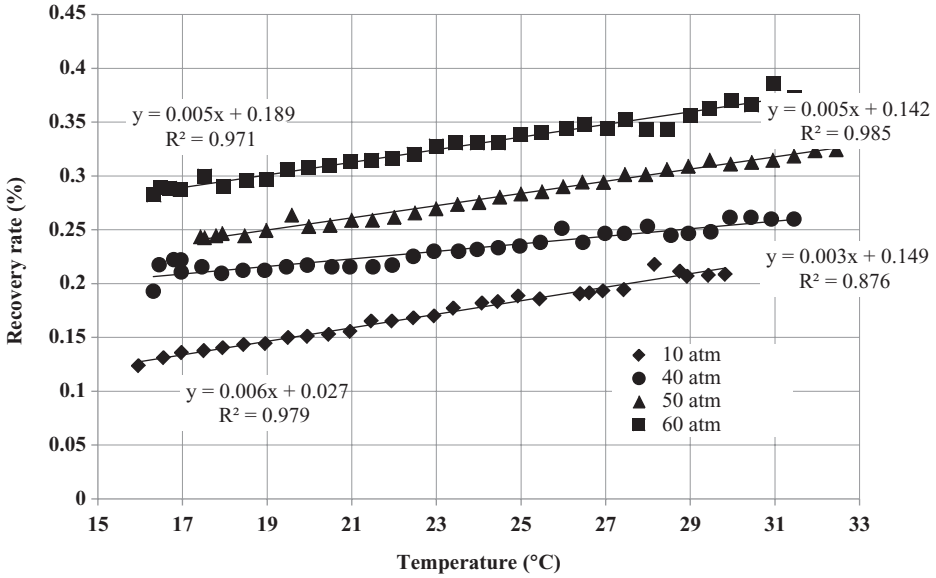

Fig. 2. Increasing recovery rate with temperature for Filmtec™ membrane at 10, 40, 50 and 60 atm. Feedwater to Reverse Osmosis unit was 0.5 M NaCl solution.

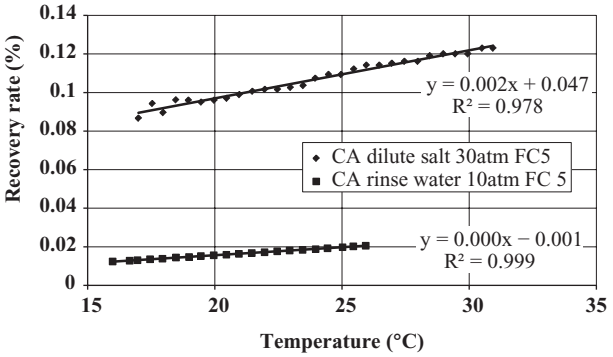

Fig. 3. Comparison of permeate flow rates against temperature for a cellulose acetate membrane at 30 atm with brackish water (0.2 M NaCl) and 10 atm with rinse water.

and Filmtec™ membranes, with increasing temperature, at a relatively low feed pressure of 10 atm and with dilute, rinse water feed, are given in Fig. 4.

These results suggest that the membrane characteristics and how each membrane reacts with temperature are markedly different to each other. The increase in permeate flux and recovery rate could be due to several factors, as discussed earlier, such as reduced viscosity and membrane pore swelling. The effect of a reduced pore water viscosity can be tested using the Hagen-Poiseuille equation (1), which predicts an inverse relation between the permeate flux and the viscosity of the pore water, for a membrane of constant geometry and at a constant applied pressure. A summary of the experiments carried out in this study show an average increase for Filmtec™ membranes of about 3%/°C in recovery rate and about 1.5%/°C in permeate flow rate, at 50–60 atm. In comparison, CA membranes gave a similar increase for both recovery rate and permeate rate, of about 2%/°C, at 30 atm. The feed flow rate was also found to change with temperature, although the effect was negligible, typically showing a decrease in feed flow of less than 0.2%/°C. The H-P equation predicts a linear change in permeate flux of about 2.4%/°C, over the 20–30°C range, using precise values for the viscosity of water, over this range. The results obtained in this study for Filmtec™ and CA membranes were therefore quite close to the value predicted by this simple macroscopic model.

Salt rejection rates may also change with temperature and so the electrical conductivities of feed and permeate samples were measured, at a constant temperature. Samples of each were taken during a standard temperature run, at 3°C intervals. These were then equilibrated in a 25°C water bath for the conductivity measurements. The mean Born energy difference between the feed water and membrane pores can then be estimated in each case using the conductivity data from the membrane separation process, in Eq. (3). For these calculations it was assumed that the NaCl concentration is proportional to the measured electrical conductivity, which is quite accurate over these concentration ranges. The values obtained for Filmtec™ and CA membranes as a function of temperature are summarized in Tables 1 and 2. The behaviour of each membrane with temperature is compared in Fig. 5. These results indicate that Filmtec™ membranes reject salt less effectively at higher temperatures, whereas CA membranes get slightly better.

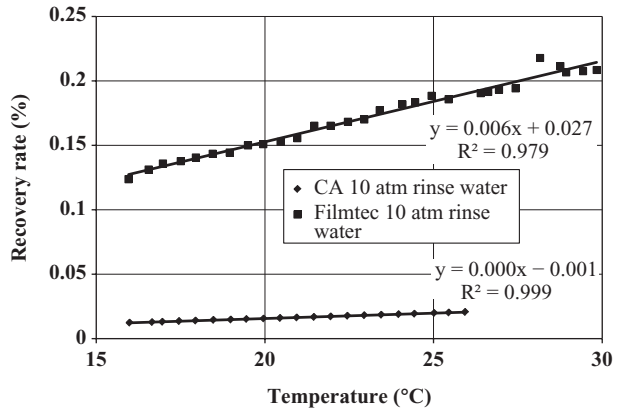

Fig. 4. Comparison of Filmtec™ and Cellulose Acetate membrane recovery rates with temperature using rinse water as feed.

From these Born energy (ΔE) values it is also possible to calculate the effective dielectric constant felt by Na^+ and Cl^- ions within the porous network of the surface skin layer of these RO membranes. Thus, the Born equation (4) can be used to estimate $\varepsilon^0{}_m$ values for the two membranes, as a function of temperature. Values for the static dielectric constant of the feed solution were obtained from the measurements of the real and imaginary components of the dielectric constant of seawater and equivalent NaCl solutions, measured at 3 GHz with temperature (6). Note that the static dielectric constant of salt solutions is significantly lower than pure water values. For example, at 20°C, the dielectric constant of water is about 80, whereas the static dielectric constant of a 0.6 M NaCl solution is about 70 [14]. These solution values were used in Eq. (4), in place of the water dielectric constant term ($\varepsilon^0{}_w$). The other parameter required in Eq. (4) is the radius of the ion. This presents an interesting problem because the passage of NaCl through the membrane is found to be symmetric, that is the pH does not change in the permeate. Hence, both ions must pass through the lower dielectric constant porous structure at about the same rate. Hence, it would seem that an 'effective' value for the radius should be used which encompasses both ions, since the ions have quite different sizes. It has been argued that experimental radii [15] should be used rather than Pauling radii [16], for solution studies. In this work we have used the geometric mean radius of the experimental values for Na^+ (0.117 nm) and Cl^- (0.164 nm), that is a value of 0.1385 nm, to estimate the effective dielectric constant of the membrane. This value is, in fact, quite similar to the geometric mean of the Pauling radii.

Using these values and the experimental data, the effective static dielectric constants of Filmtec™ and CA membranes with temperature are presented in Fig. 6. As expected, the values are significantly below the values for pure water or salt solutions. Fig. 6 indicates that Filmtec™ membranes reject salt more effectively (i.e., with a lower dielectric constant) but these membranes become less effective at higher temperatures.

A study of the effects of feed water de-gassing was carried out using CA membranes in the pilot unit, at a feed pressure of 30 atm and using a feed of 0.2 M NaCl solution. After 30 min the feed solution was degassed by passing through a hollow fibre unit attached to a high flow rate vacuum pump, running at a pressure of about 0.42 kPa, which corresponds to a de-gassing level of about 126 ppb dissolved O_2. After 60 min the vacuum pump was isolated and the system allowed to return to normal, gassed operation. Fig. 7 shows some typical results obtained on de-gassing, with the CA membranes. Typically, the permeate flux increased by about 1.5% and then decreased towards the baseline rate, when the vacuum pump was switched off.

Using Filmtec™ membranes with brackish water (at about 0.2 M NaCl), initial degassing, that is when the membrane was first exposed to a de-gassed feed, produced a more significant increase in the permeate flow rate, typically by up to 7%. Subsequent degassing runs, using the same membrane and flow characteristics, gave a lesser, further increase in permeate flow, of about 2%. In subsequent tests, the permeate flow did not increase further. An example of this behaviour is shown in Fig. 8. All experiments were run with the same applied pressure and feed water flow. Also, the final experiment on Fig. 8, labelled 'cumulative 4', was not a degassing run, instead it was the membrane operated under standard conditions. In this case, the first 6 degassing experiments, after the membrane was

Table 1
Conductivity and △E/kT data for CA membrane with temperature

Temperature (°C)	Conductivity permeate (mS/cm)	Conductivity bulk (mS/cm)	$\Delta E/kT$ ($T = 20$°C)	Change (%)
21.0080	1.853	24.38	2.5858	0.00
23.9645	1.888	24.39	2.5933	0.29
26.9565	1.909	24.00	2.5915	−0.07
29.9525	1.919	24.08	2.6154	0.92

Table 2
Conductivity and △E/kT data for Filmtec™ membrane with temperature.

Temperature (°C)	Conductivity permeate (mS/cm)	Conductivity bulk (mS/cm)	$\Delta E/kT$ ($T = 20$°C)	Change (%)
20.9945	0.794	51.0	4.1766	0.00
23.9995	0.897	51.2	4.0996	−1.84
27.06	1.009	51.3	4.0233	−1.86
29.9635	1.109	50.8	3.9544	−1.71

originally fitted, were examined. The same trend was witnessed even though the feedwater streams used for these experiments were seawater. Another example is shown in Fig. 9. It appears that exposure to degassed feed water leads to a significantly higher overall average permeate flow. Furthermore, it was also noted that once the higher overall permeate flow rate was achieved, the permeate flow appeared to show less fluctuations.

4. Discussion

Permeate flow rates and recovery rates, for both Filmtec™ and cellulose acetate membranes, measured over a wide range of feed pressures, showed a linear increase with temperature, as anticipated by the Hagen-Poiseuille equation. The overall observed relative rates of increase of recovery rate and permeate flow rate were in the range 1.5–3.0%/°C, and so are consistent with the predicted H-P slope of about 2.4%/°C, over this temperature range. This agreement is, perhaps, surprising, given the complexity of the RO process and the fact that normal viscous flow can only be an approximation to the molecular flow occurring within the RO polymer membrane matrix of nanopores.

The increase in recovery rate obtained with CA membranes at different applied feed pressures (for example, see Fig. 3) demonstrate a clear difference for the dilute feed water (at about 0.01 M NaCl) and brackish water (at about 0.2 M NaCl). The simple H-P model suggests that the effect of temperature should be the same for all membranes and feed solutions, assuming that essentially dilute salt is present in the membrane pores. Assuming a 95% salt rejection, the effective salt concentration in the pores would be less than 0.01 M. At this concentration, the viscosity will be close to that of pure water. With the more dilute feed water used in the CA experiments, the membrane water should be quite pure. Clearly, the H-P model explains most of the effect, but some of the other factors may also be involved. However, a smaller effect with temperature is unlikely to be related to many of the other effects listed earlier, simply because most of these would produce an even better improvement of permeate flux with temperature. For example, concentration polarization and the fluid boundary layer effects should both decrease with temperature, enhancing permeate flux. Simple expansion or swelling of the membrane with temperature would also increase the flux. Another factor, is that with increasing temperature the feeds for both CA and Filmtec™ membranes decreased slightly,

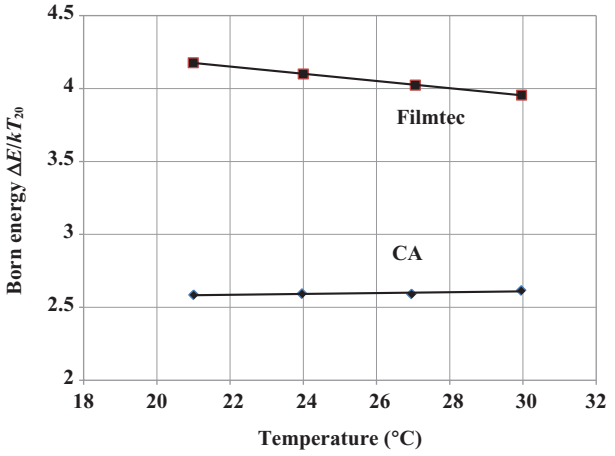

Fig. 5. Comparison of the calculated Born energy values $\Delta E/kT_{20}$ with temperature for Filmtec™ and CA membranes.

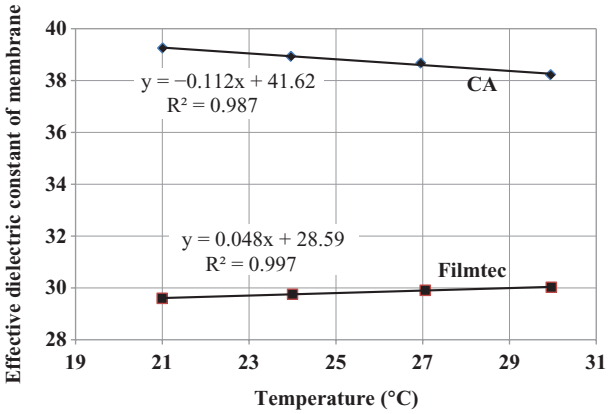

Fig. 6. Comparison of the effective static dielectric constants of Filmtec™ and CA membranes with temperature.

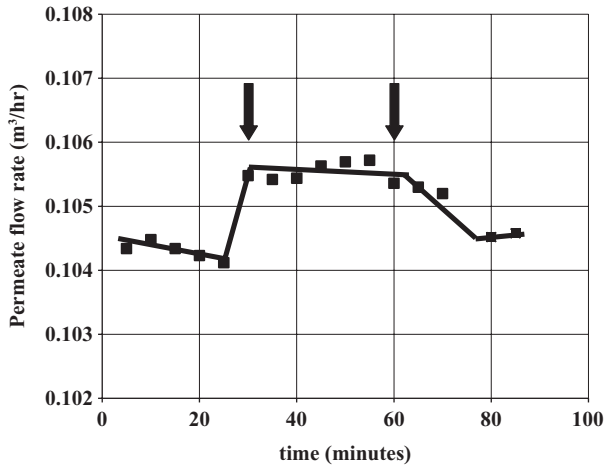

Fig. 7. Enhanced permeate flux (cumulative flow rate) upon degassing using a cellulose acetate membrane at 30 atm. The start and finish of the de-gassing period are marked with arrows.

although this effect is unlikely to have changed the permeate rate significantly.

The conductivity measurements on feed and permeate samples with temperature, for both membranes, have been analysed using the simple Born model. This compares the feed water static dielectric constant with an 'effective' calculated dielectric constant sensed by an ion of radius 0.1385 nm, representing Na^+ and Cl^- ions. The Born energy of transfer from the feed solution to the membrane is much larger for Filmtec™ membranes, which reject salts more effectively than CA membranes (see Fig. 5). As the temperature increased the Born energy ($\Delta E/kT$) values for Filmtec™ reduced at a constant rate, while the CA values remained fairly constant. These results indicate that to achieve better rejection rates, the Filmtec™ membranes should be run

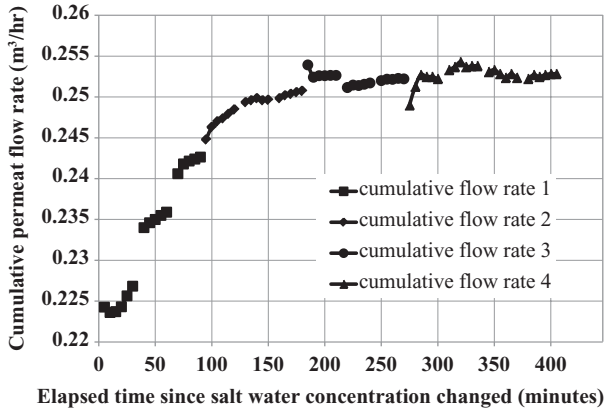

Fig. 8. Elapsed time graph, following change in salt water concentration of feed, of permeate flow for Filmtec™ membrane when first degassed.

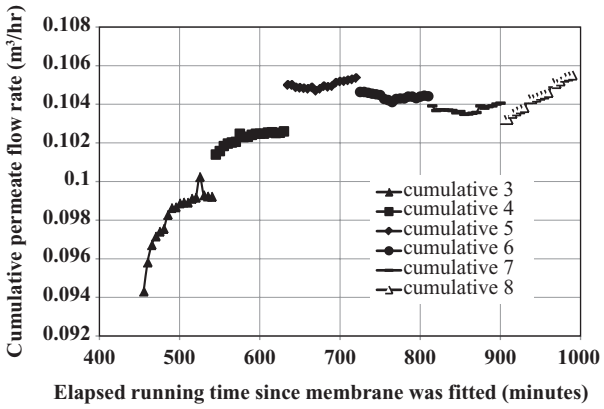

Fig. 9. Elapsed time graph of permeate flow for Filmtec™ membrane when first installed and degassed.

at the lower temperatures, but unfortunately this reduces the permeate rate. Hence we might expect the operating temperature to be a compromise between an acceptable salt rejection rate and the recovery rate. It is noteworthy that although CA membranes have a lower salt rejection level and operate at lower applied pressures, higher temperatures favour both an increased permeate flux and a better salt rejection rate, for these membranes. This can be seen more clearly when the effective static dielectric constant is calculated from the Born energy for each membrane (see Fig. 6).

Although the analysis used here for comparison purposes seems reasonable, a more accurate estimate of the dielectric constant of the membranes could be obtained using the real concentration of salt adjacent to the membrane surface, due to concentration polarisation, rather than simply the feed water concentration, as was used here. However, this surface concentration depends on many factors, such as: feed rate, feed water turbulence, rejection rate, permeate flow rate and applied pressure/osmotic pressure ratios and was not determined for the experimental conditions used in this study.

The effects of de-gassing the feed water on the permeate rate for CA membranes (see Fig. 7) show a transient increase in permeate flow rate, of 1.5%. However, over the first few months of operation, the permeate output of membranes consistently drop [17,18]. This is usually attributed entirely to compaction, however it could very likely be due in part to cavitation. This would suggest an even greater potential for improvement, with feed water degassing. There are also two other factors to consider when the feed solutions are degassed. Using the hollow-fibre vacuum system, water boils off and the temperature of the feed solution decreases, which will slightly reduce the permeate rate observed when using a de-gassed feed, due to the slight increase in viscosity. This effect could

partially mask the effects of de-gassing. In addition, the water vapour produced by the hollow-fibre degassing process, could be easily collected, as high quality water, which will help to make the process more economical.

In addition to the transient effects of de-gassing, there is increasing evidence that supports the view that, at least with Filmtec™ membranes, there is a sustained improvement of permeate flow following temporary de-gassing of the feed water. The average improvement over time for the Filmtec™ studies (see Figs. 8 and 9) was found to be up to 11%. This improvement in permeate flow is different for that observed with CA. With CA membranes, the permeate flow increases immediately upon degassing. On the other hand, the permeate flow from Filmtec™ membranes increases *over time* as degassed feedwater is pumped through the membrane. As mentioned before, this improved permeate flux will be still higher when the water that can also be collected via vacuum distillation from the hollow fibre membranes is included. This effect went unnoticed in our earlier studies, because of the gradual way the permeate flow rate increased, even when degassing ceased. By comparison, it is interesting to note that, for the CA experiments, the permeate flow was found to consistently drop back to the baseline when the vacuum pump was switched off.

5. Conclusions

The results presented here show that the simple Hagen-Poiseuille equation for flow through a capillary, gives an accurate representation of the effect of increasing temperature on the permeate rate obtained with typical RO membranes, using seawater and brackish water. A salt rejection study has demonstrated that Filmtec™ membranes become less effective as the temperature rises between 21 and 30°C, whereas Cellulose Acetate membranes actually improve over this temperature range. CA membranes showed a slight, transient improvement in permeate rate when the feed water was de-gassed. However, Filmtec™ membranes appear to show a persistent and significant improvement in permeate rate, after the membranes are exposed to de-gassed feed water. As the feedwater is currently degassed at a low level prior to reverse osmosis in industry to protect the membranes, higher rates of dissolved gas removal from the feedwater would not be difficult to implement.

Acknowledgements

The authors would like to thank Miles Rzechowicz for contributing to the data contained in Figure 9 and for constructing the schematic presented in Figure 1. The authors would also like to acknowledge Stone Ridge Ventures financial contribution in construction of the Reverse Osmosis pilot and the National Centre of Excellence in Desalination (NCED) for the use of their facilities.

Symbols

V_f	the flow rate through a pore
r	the radius
l	the length
$\triangle P$	the applied pressure gradient
η	the dynamic viscosity
$\triangle P$	effective cross membrane pressure
$\triangle P_a$	applied pressureminus the osmotic pressure at the surface of the membrane
π_m	osmotic pressure at the surface of the membrane
$\triangle E$	The Born energy difference
C_i^f	concentration of the feed solution
C_i^m	concentration of the solution within the membrane
z	the valency of the ion
q_e	the electronic charge of the ion
a	the radius of the ion
ε_0	the permittivity of free space
$\varepsilon^0{}_m$	the static dielectric constant of the membrane skin layer
$\varepsilon^0{}_w$	the static dielectric constants of the feed solution

References

[1] See commercial reports: Energy Recovery Inc. http://www.energy-recovery.com and A. A. Maghrabi, T. Green, S. Al-Ghanmdi, Effect of high feed temperature on nanofiltration and RO membrane performance: http://www.swcc.gov.sa/files%5Cassets%5CResearch%5CTechnical%20Papers%5CReverse%20Osmosis/EFFECT%20OF%20HIGH%20FEED%20TEMPERATURE %20ON%20NANOFILTRATION%20AND%20RO%20%20ME.pdf.

[2] Z.K. Al-Bahri, W.T. Hanbury and T. Hodgkiess, Optimum feed temperatures for seawater reverse osmosis plant operation in an MSF/SWRO hybrid plant, Desalination, 138 (2001) 335–339.

[3] H. Mehdizadeh and J.M. Dickson, Temperature effects on the performance of thin-film composite, aromatic polyamide membranes, Ind. Chem. Eng. Res., 28 (1989) 814–824.

[4] Filmtec™ Product Information, Form No. 609-00377-0406, Dow, 2008. Dow Liquid Separations, Technical Manual on FILMTEC™ Membranes. http://www.Filmtec™.com.

[5] R.E. Kesting, Synthetic Polymeric Membranes: A Structural Perspective, 2nd ed., John Wiley & Sons, New York, 1985.

[6] M. Mulder, Basic Principles of Membrane Technology, Kluwer Academic Publications, 1991.

[7] S. Sourirajan, Reverse Osmosis, Academic Press, New York, 1970.

[8] E. Colin, W. Clarke and D.N. Glew, Evaluation of the thermodynamic function for Aqueous Sodium Chloride from equilibrium and calorimetric measurements below 154°C, J. Phys. Chem. Ref. Data, 14 (2) (1985) 489–610.

[9] P. Atkins and J. De Paula, Physical Chemistry, 8th ed., Oxford University Press, 2006, pp. 110–111.

[10] W. Ellison, A. Balana, G. Delbos, K. Lamkaouchi, L. Eymard, C. Guillou and C. Prigent, New permittivity measurements of seawater, Rad. Sci., 33 (3) (1998) 639–648.
[11] M. Rzechowicz and R.M. Pashley, The effect of de-gassing on the efficiency of Reverse Osmosisfiltration, J. Mem. Sci., 295 (2007) 102–107.
[12] M.J. Francis, R.M. Pashley and M. Rzechowicz, The effects of feedwater de-gassing on the permeate flux of a small scale SWRO pilot plant, Desal. Wat. Treat. 25 (2011) 150–158.
[13] Technical Information Cerabar S PMC71, PMP71, PMP75 Process pressure measurement. Endress + Hauser Instruments International AG https://wa001.endress.com/dla/50002188824/000/03/TI383PEN_0808.pdf accessed 11/5/2010
[14] R.A. Robinson and R.H. Stokes, Electrolyte Solutions, Butterworths, London, 1955.
[15] M.J. Blandamer and M.C.R. Symons, Significance of new values for ionic radii to solvation phenomena in aqueous solution, J. Phys. Chem., 67(6) (1963) 1304–1306.
[16] L. Pauling, The Nature of the Chemical Bond and the Structure of Molecules and Crystals, 3rd ed., Cornell University press, Ithaca, New York, 1960.
[17] H. Mehdizadeh and J.M. Dickson, Modelling of temperature effects on the performance of Reverse Osmosis membranes, Chem. Eng. Comm., 103 (1) (1991) 99–117.
[18] S. Kumira and S. Sourirajan, Performance of porous cellulose acetate membranes during extended continuous operation under pressure in reverse osmosis process using aqueous solutions, Ind. Chem. Eng. Proc. Des. Dev., 7(2) (1968) 197–206.